

Investigation of Poincare Solutions of Nonlinear Duffing Oscillator under Varying Beats Using Fractal Disk Characterisation

Lawal O. Raphael¹, Tajudeen A. O. Salau¹, Azeez. A. Adebayo^{1,2},
Seiyefa A. Vincent¹

Department of Mechanical Engineering, University of Ibadan, Nigeria¹; Auburn University, USA²

Corresponding Author: Azeez. A. Adebayo (azeezadebayo39@gmail.com; aaa0084@auburn.edu)

Received 25 June 2023; Accepted 21 July 2023

Abstract: This research investigates the effect of varying beats on the steady Poincare solutions of nonlinear duffing oscillator. A non-dimensional second order differential equation based on the general governing equation for nonlinear duffing is presented and solved numerically using the fourth order Runge-Kutta method. The fractal disk method is used to characterize the Poincare solutions, and scatter plots of the oscillator per unit space area show chaotic and non-uniform distributions. Qualitatively, it is observed that the Poincaré solutions for Duffing oscillators subject to harmonic excitation are visually similar to those obtained at zero beat value. However, upon closer examination, differences in dimensions become apparent. Specifically, the Duffing system under harmonic excitation yields an estimated dimension value of 1.346 ± 0.02 , whereas the dimension for the Duffing system under zero beat conditions is determined to be 1.368 ± 0.06 , resulting in a difference of 1.65%. The variation in beats distorts the Poincare diagrams and dimensions, with beat values of -5%, -2%, 3%, and 5% resulting in dimensions that are different from the zero beats dimension by 9.93%, 6.30%, 22.27%, and 14.78%, respectively. Overall, this research provides insights into the behavior of nonlinear duffing oscillators under varying beats.

Keywords: Nonlinear duffing oscillator, beats, Poincare solutions, fractal disk method.

I. INTRODUCTION

Nonlinear oscillators have been extensively studied in various fields, including physics, engineering, and mathematics, due to their relevance in modeling complex systems. The nonlinear Duffing oscillator is a prominent example that exhibits complex behavior under certain conditions [1][2]. Harmonic excitation of the Duffing oscillator can result in chaotic responses under certain drive parameter combinations [3]. However, the impact of varying beats on the steady-state Poincare solutions of this oscillator has not received much attention in the literature.

Nonlinear dynamical systems are ubiquitous in science and engineering, and their behavior is often complex and difficult to analyze mathematically [4]. Numerical methods provide powerful tools for solving these systems, allowing researchers to investigate their behavior and make predictions about their future evolution [5]. One commonly used approach is the numerical integration of differential equations, where the equations of motion are discretized and solved iteratively [6]. Other methods, such as the shooting method and finite difference methods, can also be used to solve nonlinear dynamical systems [7]. The application of numerical methods to nonlinear dynamical systems has been a subject of active research in recent years [8]. A deep neural network method for solving high-dimensional nonlinear dynamical systems was proposed by [9] while [10] proposed a hybrid numerical method for solving nonlinear systems with both smooth and nonsmooth functions. Another recent development is the use of machine learning techniques, such as reinforcement learning, to optimize the performance of numerical solvers for nonlinear dynamical systems. Numerical methods have been applied to a wide range of problems in physics, biology, chemistry, and engineering. For example, in fluid mechanics, numerical simulations are used to study turbulent flows and complex fluid dynamics [11]. In biology, numerical methods have been used to model the spread of infectious diseases and the growth of cancer tumors [12]. In engineering, numerical methods are used to optimize the design of structures and mechanical systems, such as aircraft wings and wind turbines [13].

Recent studies have shown that fractal analysis is a promising tool for studying the behavior of nonlinear systems, including oscillators [14]. Fractal analysis quantifies the self-similarity and complexity of a system and has been applied to characterize the Poincare solutions of nonlinear duffing and pendulum oscillators under periodic excitations [15]. Fractals are mathematical objects that display the same pattern at every scale and are often described as manifolds without differentiability [16]. Unlike Euclidean geometry, which struggles to analyze

complex and rough shapes, fractal geometry can accommodate all the complex shapes that exist in the real world [17]. Examples include trees, coastlines, cloud formations, leaf venations, fruit shapes, and voice signals. Fractal geometry is not limited to the unnatural shapes of Euclidean geometry. Fractals can be broken down into smaller versions of themselves, with each part being a copy of the entire pattern. This phenomenon of self-similarity describes how a small fragment of a fractal resembles a larger piece or even the entire object when examined. Fractals are commonly used in computer modeling to reproduce irregular patterns and structures found in nature because they produce irregular shapes and surfaces through the repetition of geometric patterns at smaller and smaller scales, which classical geometry cannot represent [18].

The present study aims to investigate the effect of varying beats on the steady Poincare solutions of nonlinear Duffing oscillators using the fractal disk method for characterization. The study builds on recent works by [15] and [19] who have characterized the behavior of nonlinear systems, including duffing and pendulum oscillators under selected periodic excitations with fractal disk and Gram-Schmidt orthogonalized lyapunov exponents respectively. The use of fractal analysis in this study provides a more detailed understanding of the behavior of nonlinear Duffing oscillator under varying beats and offers insights into the potential applications of fractal analysis in nonlinear dynamics, chaos theory, and control systems.

II. METHODOLOGY

Duffing Equation

The current research utilized a pre-existing simplified version of the duffing equation (2.1). This equation is expressed in a dimensionless form to reduce the number of adjustable parameters involved [15].

$$\ddot{x} + \gamma\dot{x} - \frac{x}{2}(1-x^2) = P_0 \sin(\omega_D t) \tag{2.1}$$

The symbols x , \dot{x} , and \ddot{x} correspond to the oscillator's displacement, velocity, and acceleration with respect to a reference point. The degree of damping in the system is controlled by the parameter γ . The amplitude strength of the harmonic excitation is denoted by P_0 , while the excitation frequency is represented by ω_D . The variable t signifies the time.

Beat Phenomenon in Duffing Oscillator

To Simulate the beat phenomenon in a duffing set up, a single equation representing the two super-imposed waves was generated from the addition of two harmonic functions. The two waves were similar but non-identical as a result of a difference in frequency.

For the Duffing Equation; the Harmonic Functions representing the waves were

$$x_1 = P_0 \sin \omega_1 t \tag{2.2.1}$$

$$x_2 = P_0 \sin \omega_2 t \tag{2.2.2}$$

Where;

$$|\omega_2 - \omega_1| = b, \quad \omega_1 \approx \omega_2, \quad b = \text{beat value}$$

$$\therefore \omega_2 = \omega_1 + b \tag{2.2.3}$$

Combining both wave equations 2.2.1 and 2.2.2 the equation below was obtained;

$$x_1 + x_2 = P_0 \sin \omega_1 t + P_0 \sin \omega_2 t \tag{2.2.4}$$

Substituting the value of equation (2.2.3) into equation (2.2.4) we obtained;

$$x_1 + x_2 = P_0 \sin \omega_1 t + P_0 \sin(\omega_1 + b)t \tag{2.2.5}$$

Referring to the Trigonometry relation;

$$\sin A + \sin B = 2 \sin\left(\frac{A+B}{2}\right) \cos\left(\frac{A-B}{2}\right) \tag{2.2.6}$$

$$P_0 \sin \omega_1 t + P_0 \sin(\omega_1 + b)t = 2P_0 \sin\left(\frac{\omega_1 t + \omega_1 t + bt}{2}\right) \cos\left(\frac{\omega_1 t - \omega_1 t - bt}{2}\right)$$

$$= 2P_0 \sin\left(\frac{2\omega_1 t + bt}{2}\right) \cos\left(\frac{-bt}{2}\right) \tag{2.2.7}$$

Rescaling the term to have the same strength as the Excitation amplitude of the individual waveforms;

$$x_1 + x_2 = \frac{1}{2} \times 2P_0 \sin\left(\omega_1 + \frac{b}{2}\right)t \cos\left(\frac{b}{2}\right)t \tag{2.2.8}$$

The beat value b , is represented as a percentage of ω_1 and the qualitative descriptions are shown below.

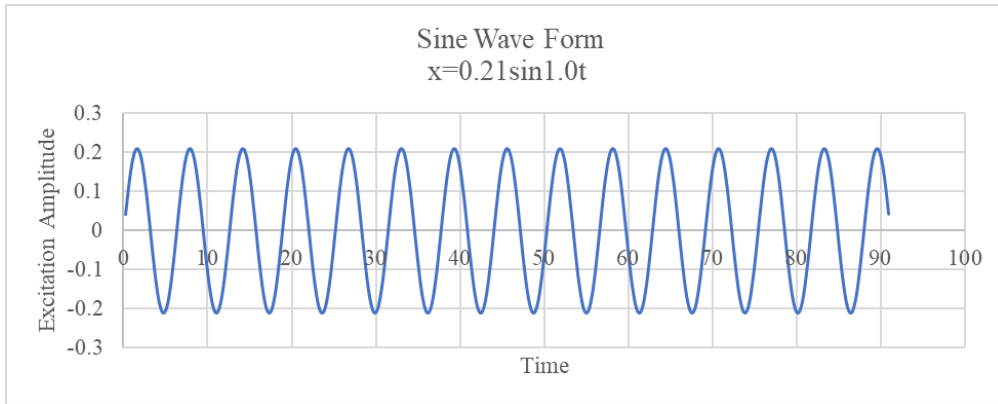


Figure 2.1: sine wave form of equation 2.2.1

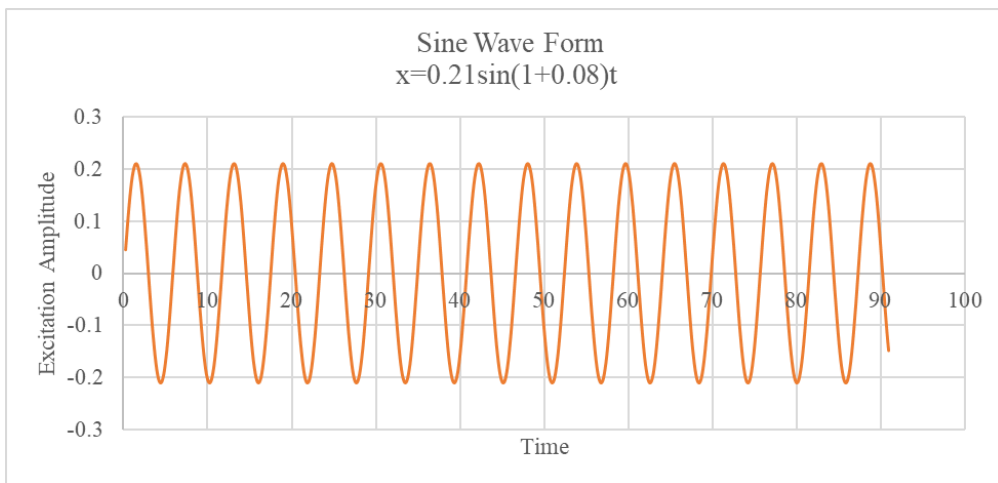


Figure 2.2: sine wave form of equation 2.2.2

Combined Wave Form

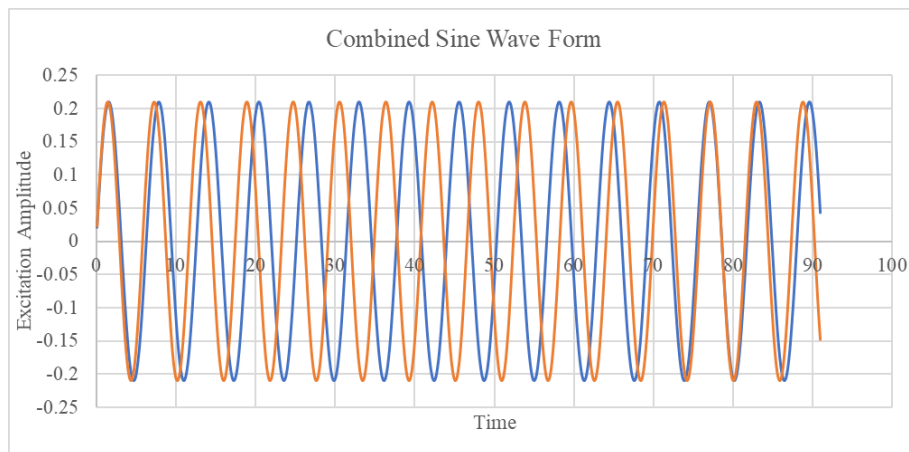


Figure 2.3: Superposing of the Two Similar Waves (i.e. from figures 2.1 and 2.2)

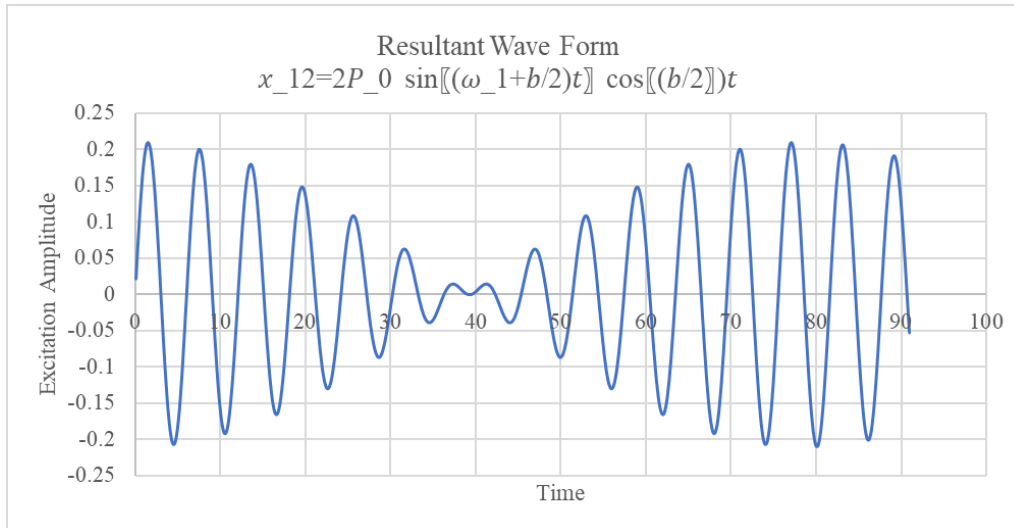


Figure 2.4: Resultant of the Two Superposed Waves represented by equation 2.2.8

Fourth-Order Runge-Kutta Scheme

The present study utilized the popular constant operation time step fourth order Runge-Kutta schemes to simulate equation (1) in the transformed pair of first order rate equations. The respective details of the scheme are provided in equations (2.3.1) to (2.3.4) substituting y for (θ_1, θ_2) , x for (t) and constant time step h .

$$y_{i+1} = y_i + \frac{h}{6} [K_1 + 2(K_2 + K_3) + K_4] \quad (2.3)$$

$$K_1 = f(x_i, y_i) \quad (2.3.1)$$

$$K_2 = f\left(x_i + \frac{h}{2}, y_i + \frac{hK_1}{2}\right) \quad (2.3.2)$$

$$K_3 = f\left(x_i + \frac{h}{2}, y_i + \frac{hK_2}{2}\right) \quad (2.3.3)$$

$$K_4 = f(x_i + h, y_i + hK_3) \quad (2.3.4)$$

Study parameters

Duffing Oscillator

From literature research, this study focuses on the parameters defined by; the non-dimensional forcing amplitude ($P_0=0.168$), damping constant ($\gamma=0.21$). Simulation of these parameters was carried out over the drive frequency $\omega_D = 1$. The simulation time step is fixed at $h = \frac{T_P}{500}$ for $T_P = \frac{2\pi}{\omega_D}$ and the initial conditions for studied cases is $(0, 0)$. The simulation was executed for 2000-excitation periods (i.e. $50T_P - 2050T_P$).

Characterization Methods

The fractal characterization method used was the disk count method.

A brief description of how the process was carried out in the computer code developed for fractal analysis is given. The procedure essentially consisted of the following steps:-

- (i) Determining the characteristic length of the Poincaré shape
- (ii) Determining the size of the disk to be used in covering the figure based on the zooming or resolution
- (iii) Completely covering the shape with disks of the size determined in the step (ii)

- (iv) Counting the number of disks required to complete step (iii) a number of times and taking note of the optimum count figure (number)
- (v) Repeating steps (iii) and (iv) for ten levels of zooming or resolutions (from 1 to 10)
- (vi) Tabulating from resolution level 1 to 10 and making a log-log plot of the resolution level against the optimum number of disks required to completely cover the figure (scatter plots)
- (vii) Taking the slope of the log-log plot and assigning it as the fractal dimension of the figure.

All of steps (i) to (vii) were carried out in code with the only contact with the program being the inputting of the parameter combination at the beginning of the code run, and the collection of the fractal dimension number at the end of the code run.

Using the Disk count method, the result of the fractal analysis was a decimal between 0.0 and 2.0. This is because the Poincaré section for the system response of this study was embedded in 2-dimensional space. The guideline for characterization for a fractal embedded in 2-dimensional space is based on number values and is stated here. A fractal dimension number that is equal to 0.0 denotes periodic response. A fractal dimension number that is greater than 0.0 but less than one 1.0 denotes response that is no longer periodic but not yet chaotic (could be period doubling, quasi-periodic, period two, period-three, e.t.c). A fractal dimension number that is greater than 1.0 denotes chaotic response, with the degree of chaos increasing with larger fractal dimension numbers.

Fractal dimension can be obtained with the mathematical equation given as

$$Y \propto X^D \tag{2.5}$$

Proportional related equation (2.5) can be re-written as

$$Y = KX^D \tag{2.5.1}$$

X = Number of Disks (same size) used to overlay the characteristic length (AB) of a fractal image in 2-dimensional Euclidean space.

Y = Number of Disk required to overlay fractal image with corresponding characteristic length (AB) in 2-dimension Euclidean space.

D = Fractal dimension. This will be referred in this study as Estimated Disk dimension for Disk count method.

K = Constant of proportionality

Take natural logarithm (any base) of both sides of equation (2.5.1) to make it a linear function, this yields

$$\ln(y) = D\ln(x) + \ln C \tag{2.5.2}$$

Rewrite equation (2.5.2) simply as (2.5.3)

$$y = Dx + C \tag{2.5.3}$$

An algorithm based on Disk count method and incorporated with equation (2.5.3) was developed to enable the estimation of dimension for selected fractals of this study using least square regression schemes. The algorithm was coded in FORTRAN language and can compute transient and steady solutions of fractals (scatter plots of Poincare results) and Disk count method.

III. RESULTS AND DISCUSSION

Comparison of the result with literature

Duffing Oscillator

Comparison was done in the validation step for the Poincaré sections, firstly under harmonic excitation. The Poincare patterns in figure 3.2 compare excellently well with those reported by [20], amplitude ($P_o = 0.168$), damping constant ($\gamma = 0.21$) fixed drive frequency ($\omega=1$) in figure 3.1.

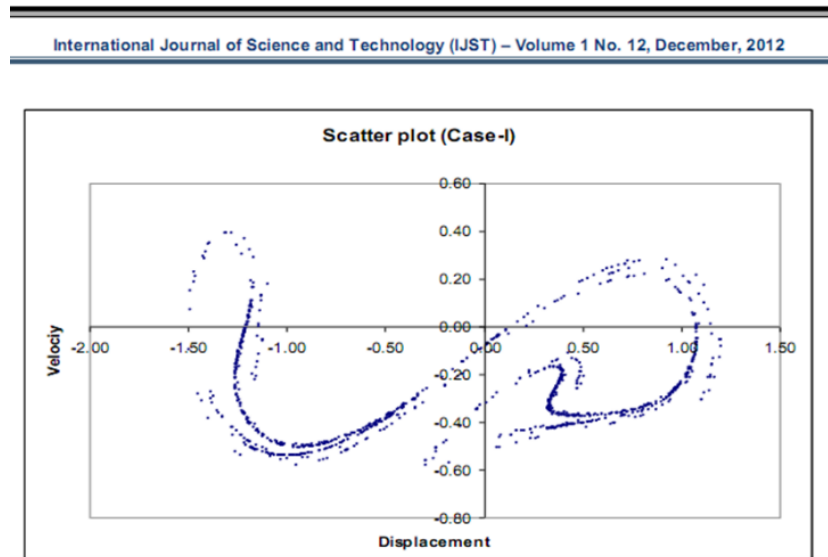


Figure 3.1: Scatter plot diagram of Duffing Oscillator at ($\omega_D = 1, \gamma=0.168$ and $P_o = 0.21$) [20]

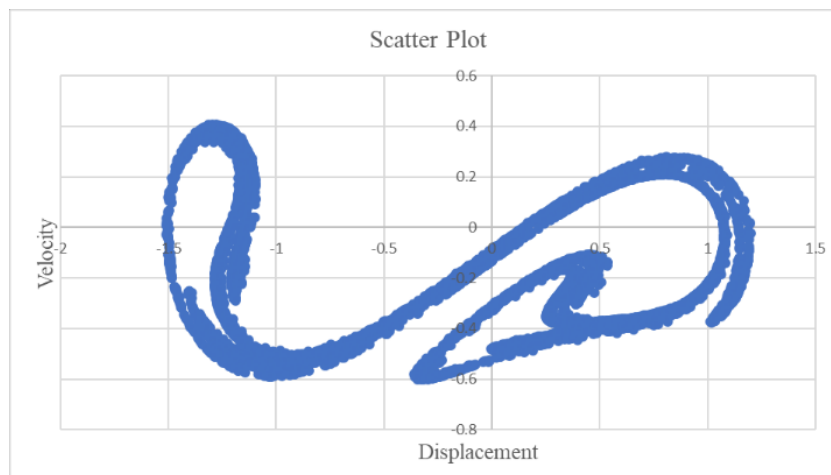


Figure 3.2: Scatter plot diagram of Duffing Oscillators at ($\omega_D = 1.0, \gamma=0.168$ and $P_o = 0.21 b = 0.0$)

Validation of code using published poincare results

Duffing Oscillator

Figure 3.3 shows Poincare solutions of harmonically excited duffing covered with disk size of 2 and 3 respectively. Figure 3.4 shows the Poincare solutions (scatter plots), with attractor layout of duffing oscillator under beat value of 1% using disk scale of 2 and 3 respectively. The scatter plots distribution per unit space area varies non-uniformly from one location to another. This shows that nonlinear duffing oscillators under varied beat value are chaotic. Tables 3.1 and 3.2 show the variation of optimum counted disks with increasing observation scale number for the referenced harmonic excitation and the periodic excitation (beat value of 1%) respectively.

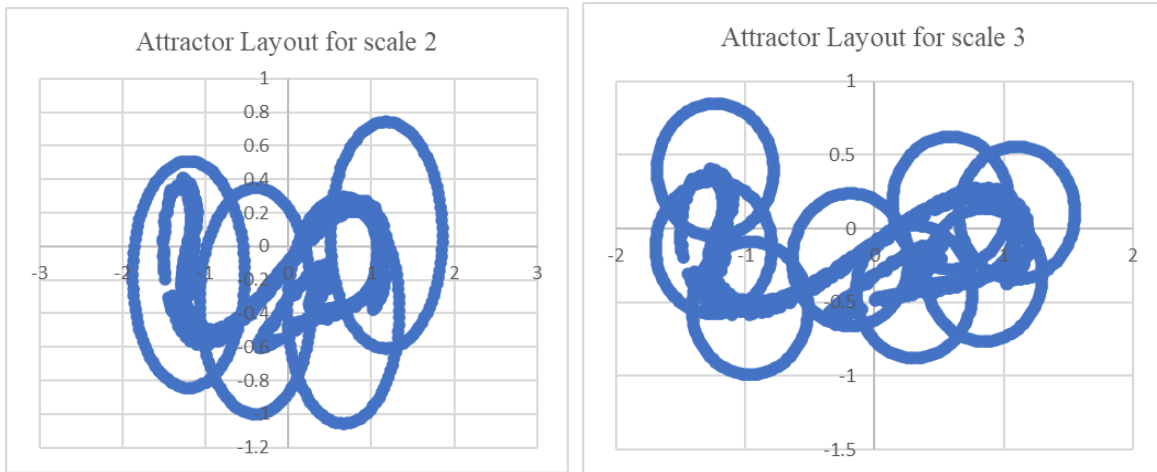


Figure 3.3: Poincare section of harmonically excited duffing oscillator showing the attractor layout for scale 2 and scale 3 disks

Table 3.1: The generated report (10 trials) of disk laying of the Poincare (harmonic excitation)

Scale	Optimum disk count	Trial 1	Trial 2	Trial 3	Trial 4	Trial 5	Trial 6	Trial 7	Trial 8	Trial 9	Trial 10
1	2	2	3	2	2	2	2	2	2	2	2
2	4	6	5	4	5	5	4	4	5	4	5
3	8	9	8	8	9	9	8	8	8	9	8
4	12	12	12	14	12	12	13	15	12	12	12
5	16	17	20	19	18	16	19	17	18	17	18
6	21	23	24	23	21	22	22	23	21	22	23
7	23	28	28	27	23	27	28	27	28	29	26
8	29	32	31	32	33	33	30	33	34	34	29
9	36	36	40	40	39	39	37	40	38	38	38
10	40	41	45	40	44	46	41	41	45	43	44

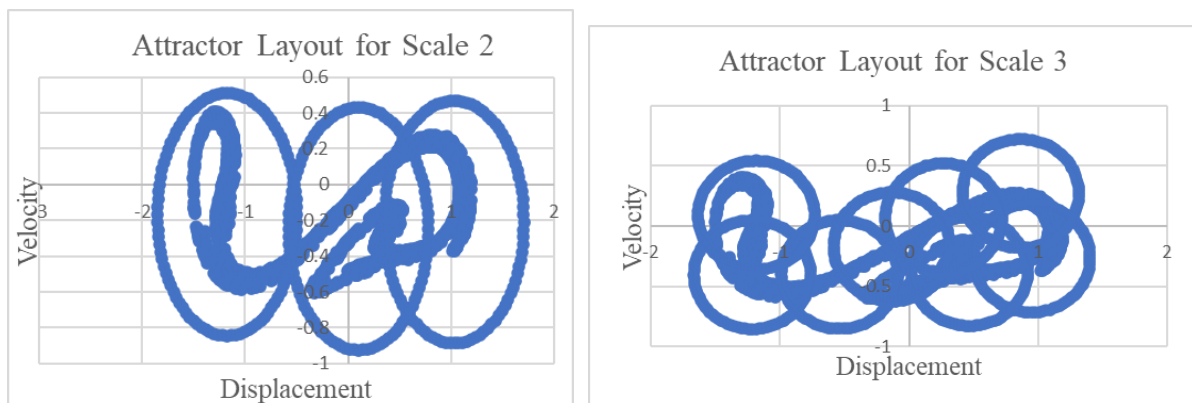


Figure 3.4: Poincare section of duffing Oscillators (at zero beat) showing the attractor layout for scale 2 and scale 3 disks

Table 3.2: The generated report (10 trials) of disk laying of the Poincare (1% beat value)

Scale	Optimum Disk Count	Trial 1	Trial 2	Trial 3	Trial 4	Trial 5	Trial 6	Trial 7	Trial 8	Trial 9	Trial 10
1	2	2	2	2	2	2	2	2	2	2	2
2	4	4	4	4	6	5	4	4	4	5	5
3	9	9	9	10	10	10	10	10	9	11	10
4	12	12	13	14	13	14	14	13	14	17	13
5	18	22	19	21	19	18	22	21	19	19	21
6	24	26	28	27	29	24	29	27	29	28	26
7	32	33	34	33	37	32	33	34	33	33	33
8	36	44	41	40	41	39	38	39	40	36	39
9	48	50	49	49	50	50	50	48	54	50	53
10	53	56	57	62	53	58	58	63	56	55	57

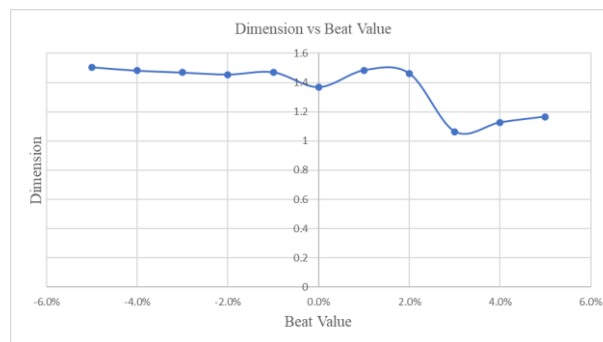


Fig 3.5: Graph of Dimension plotted against beat value for a range of 0% to 5%

Fig 3.5, shows the relationship between the variance in beat value and the Dimension of the Poincare Results. Qualitatively, the Poincaré results of Duffing oscillators subjected to harmonic excitation resemble those obtained at zero beat value. However, upon characterizing the results, differences in dimensions are observed. The dimension estimated for the Duffing system under harmonic excitation is 1.346 ± 0.02 , while the dimension for the Duffing system at zero beats is 1.368 ± 0.06 , resulting in a difference of 1.65%. This suggests that the harmonic excitation introduces subtle changes in the system's dynamics.

Furthermore, as the beat value is gradually varied, the qualitative appearance of the Poincaré diagram undergoes further distortion. The dimensions also undergoes changes, but in a non-systematic pattern. For beat values of -5%, -2%, 3%, and 5%, the dimensions of the Poincaré results are found to be 1.505 ± 0.03 , 1.455 ± 0.02 , 1.063 ± 0.09 , and 1.167 ± 0.06 , respectively. These values deviate from the dimension obtained at zero beats by 9.93%, 6.30%, 22.27%, and 14.78%, respectively.

IV. CONCLUSION

The study demonstrates that varying the beat value in the Duffing system leads to non-systematic distortions in the Poincaré results. The changes in dimensions and the qualitative appearance of the Poincaré diagram indicate that even small variations in the beat value can have a notable impact on the system's behavior. These findings highlight the sensitivity of the Duffing system to changes in the excitation conditions and emphasize the need for further investigation to understand the underlying mechanisms driving these complex dynamics.

REFERENCES

- [1]. Hilborn, R. C. (2000). Chaos and nonlinear dynamics: an introduction for scientists and engineers. Oxford University Press on Demand.
- [2]. He, J. H., Hou, W. F., Qie, N., Gepreel, K. A., Shirazi, A. H., and Mohammad-Sedighi, H. (2021). Hamiltonian-based frequency-amplitude formulation for nonlinear oscillators. Facta Universitatis, Series: Mechanical Engineering, 19(2), 199-208.

- [3]. John, J. T., Salau, T. A. O., Ayegbeso, D. O., and Adebayo, A. A. (2022). Development and Comparative Analysis of Chaos Diagram for Harmonically Excited Duffing Oscillator Using Gram-Schmidt Orthogonal Based Lyapunov Exponent. *IOSR Journal of Mechanical and Civil Engineering (IOSR-JMCE)*, 19(4), 58-66.
- [4]. Wang, W. X., Lai, Y. C., & Grebogi, C. (2016). Data based identification and prediction of nonlinear and complex dynamical systems. *Physics Reports*, 644, 1-76.
- [5]. Brunton, S. L., Budišić, M., Kaiser, E., and Kutz, J. N. (2021). Modern Koopman theory for dynamical systems. arXiv preprint arXiv:2102.12086.
- [6]. Mazumder, S. (2015). Numerical methods for partial differential equations: finite difference and finite volume methods. Academic Press.
- [7]. Dednam, W., and Botha, A. E. (2015). Optimized shooting method for finding periodic orbits of nonlinear dynamical systems. *Engineering with Computers*, 31, 749-762.
- [8]. Pappalardo, C. M., and Guida, D. (2017). Adjoint-based optimization procedure for active vibration control of nonlinear mechanical systems. *Journal of Dynamic Systems, Measurement, and Control*, 139(8).
- [9]. Han, J., Jentzen, A., and E, W. (2018). Solving high-dimensional partial differential equations using deep learning. *Proceedings of the National Academy of Sciences*, 115(34), 8505-8510.
- [10]. Luo, Y. Z., Tang, G. J., and Zhou, L. N. (2008). Hybrid approach for solving systems of nonlinear equations using chaos optimization and quasi-Newton method. *Applied Soft Computing*, 8(2), 1068-1073.
- [11]. Sahoo, A. K., and Chakraverty, S. (2022). Machine intelligence in dynamical systems:\A state- of- art review. *Wiley Interdisciplinary Reviews: Data Mining and Knowledge Discovery*, 12(4), e1461.
- [12]. Khaliq, R., Iqbal, P., Bhat, S. A., and Sheergojri, A. R. (2022). A fuzzy mathematical model for tumor growth pattern using generalized Hukuhara derivative and its numerical analysis. *Applied Soft Computing*, 118, 108467.
- [13]. Abd Elaziz, M., Elsheikh, A. H., Oliva, D., Abualigah, L., Lu, S., and Ewees, A. A. (2021). Advanced metaheuristic techniques for mechanical design problems. *Archives of Computational Methods in Engineering*, 1-22.
- [14]. He, J. H., Moatimid, G. M., and Zekry, M. H. (2022). Forced nonlinear oscillator in a fractal space. *Facta Universitatis, Series: Mechanical Engineering*, 20(1), 001-020.
- [15]. Adebayo, A. A., Salau, T. A. O., J John, T., and Musa, F. A. (2022). Investigation of Poincare Solutions of Nonlinear Duffing and Pendulum under Selected Periodic Excitations Using Fractal Disk Characterisation. *Current Journal of Applied Science and Technology*, 41(25), 1-16.
- [16]. Ng, T. T., Chang, S. F., Hsu, J., Xie, L., and Tsui, M. P. (2005, November). Physics-motivated features for distinguishing photographic images and computer graphics. In *Proceedings of the 13th annual ACM international conference on Multimedia* (pp. 239-248).
- [17]. Mandelbrot, B. B., and Mandelbrot, B. B. (1982). *The fractal geometry of nature* (Vol. 1). New York: WH freeman.
- [18]. Salau, T. A. O., and Ajide, O. O. (2013). ANovel GRAPHIC PRESENTATION AND FRACTAL CHARACTERISATION OF POINCARÉ SOLUTIONS OF HARMONICALLY EXCITED PENDULUM. *International Journal of Advances in Engineering & Technology*, 6(3), 1299-1312.
- [19]. Ayegbeso, D. O., Salau, T. A. O., John, T. J., and Adebayo, A. A. (2022). Categorization of the Behaviour of A Duffing Oscillator (Subjected To Periodic Excitations) Using Gram-Schmidt Orthogonalized Lyapunov Exponents. *IOSR Journal of Engineering (IOSRJEN)*, 12(7), 41-47.
- [20]. Salau, T.A.O. and Ajide, O.O. (2012). Investigation of Excited Duffing's oscillator Using Versions of Second Order Runge-Kutta methods, *International Journal of Science and Technology (IJST)*, Volume 1, No.12, pp.679-687